Stochastic performance assessment on long-term behavior of multilateral closed deep geothermal systems

Morteza Esmaeilpour [a],*, Maziar Gholami Korzani [b], Thomas Kohl [a]

[a] *Institute of Applied Geosciences, Karlsruhe Institute of Technology, Karlsruhe, Germany*
[b] *School of Civil & Environmental Engineering, Queensland University of Technology, Queensland, Australia*

ARTICLE INFO

ABSTRACT

Increasing the contribution of geothermal systems to green energy generation requires designing new innovative systems producing a significant amount of thermal power in a sustainable manner. The focus of this study is the performance evaluation of multilateral closed deep geothermal (MCDG) systems as a novel environmentally friendly approach for energy extraction from earth. The investigations on these synthetic systems assume a probabilistic number of borehole sections with several vertical and horizontal wellbores connected through some manifolds and doglegs. To reduce possible thermal losses, the circulated fluid is extracted through only one production wellbore. The findings of this study demonstrated that the heat absorption per meter of MCDG systems is much higher than for simple closed geothermal systems (CDG). Operating with these systems will not necessarily yield better performance. It is also found that the long-term performance of MCDG systems can be predicted as a function of their short-term behavior through stochastic analysis. This correlation is interestingly independent of the number of wellbores and flow rate. By defining specific criteria, the high-performance MCDG systems can be filtered to demonstrate common features as a specific relation between flow rates per vertical and horizontal wellbores. This characterization of MCDG systems should support the design of future high-performance systems.

1. Introduction

Utilizing geothermal energy is a clean and sustainable way of supplying thermal energy required for district heating purposes [1–3]. In contrast to other renewables (e.g., solar and wind energy), geothermal energy - extracted from the earth through open and closed systems - provides baseload power available throughout the whole year [4]. Open systems are characterized by the direct contact between circulating fluid and hot rock, while faults and fractures provide extensive heat exchange surfaces and enhance the capability of these systems for extracting a large amount of thermal power [5–7]. These systems need to be managed with care not to harm the environment or to create induced seismic events [8–10]. Fluid circulation in closed geothermal loops prevents the potential hazards [11], but the generated thermal power is much lower, making it difficult to respond to the total heating demand. Increasing the contribution of geothermal energy to the global renewable capacity necessitates developing new innovative systems that combine the advantages of both open and closed systems. Optimizing the generated thermal power of closed systems requires a specific design

of possible geometries and wellbore diameters to enhance the lateral heat exchange area and the heat absorption rate. However, these conditions often conflict with economic considerations. Herein, pathways are demonstrated to maximize energy extraction from closed geothermal systems.

In the previous study conducted by the authors of this study [12], the power production feasibility of closed-loop deep geothermal (CDG) systems with a lengthy horizontal extension was assessed. It is disclosed that a CDG system can produce an average thermal power of ~2 MW$_t$ nearly constantly over 100 years (continually) only supported by the thermosiphon effect. The longevity of this system (i.e., stability of extraction temperature over time) is also much better than those of open geothermal systems [12]. In spite of the relatively large power generation of CDG systems, their economic feasibility suffers from the small ratio of produced thermal power per length of the drilled wellbores. This could extend the payback period and may discourage the interest of investors in these closed systems. Now, this study investigates *possible novel solutions for multilateral CDG (MCDG) systems*, to increase the ratio of generated thermal power to the total length of the system by

introducing several (parallel) injection and horizontal wellbores.

The performance of open multilateral systems has been evaluated in recent studies [13–16]. However, to the best of our knowledge, assessment of the reliability of closed multilateral frameworks for district heating purposes is rarely addressed in the literature. Professional companies are already proposing to install multilateral structures without revealing details of their projects. In 2020, Wang et al. [17] investigated the production characteristics of various coaxial closed-loop geothermal systems (CCGS), leading to potential thermal power production of 3.05 MW$_t$, which is remarkably higher than those of single vertical and horizontal coaxial systems. Nevertheless, producing roughly 3 MW$_t$ power hardly compensates for the drilling expenses of a deep multilateral system possessing a vertical section with a depth of 4500 m and several horizontal wellbores with lengths of 2000 m. In another study [18], they tried to analyze the heat extraction mechanism of the CCGS. Based on their investigations, the reservoir temperature has a considerable effect on the heat extraction process that mainly occurs in the lateral wellbores of a multilateral CCGS. Since they take a formation temperature of 236 °C at 3750 m depth (i.e., assuming temperature gradients of approx. 0.06 °C/m), it is difficult to generalize the results of this study to other thermal situations.

Although few studies evaluated the performance of multilateral closed systems, they only focused on coaxial structures. However, as mentioned before, the required large wellbore diameter, heat absorption by steel connectors, difficulties in the deepening of the wellbores, and the limited range of generated thermal power are the main disadvantages of the multilateral CCGS. Therefore, MCDG systems seem to be more reliable, practical, and efficient rather than the multilateral CCGS. The present investigation of MCDG systems contributes to the existing body of knowledge having a nearly probabilistic number of borehole vertical and horizontal wellbores sections.

1. A total of 160 geometries are taken to identify a meaningful correlation between the long-term performance of MCDG systems and their short-term behavior independent of the number of wellbores and flow rate. The provided stochastic analysis forecasts the probability of various outcomes (i.e., extraction temperature, generated thermal power, and specific power) under different conditions, using random variables. In this analysis, the randomness is attributed to more than one arbitrary variable (i.e., flow rate and the number of wellbores).

2. Several measures, such as the ratio of produced thermal power to the equivalent total length (i.e., simplified/normalized indicator for drilling expenses), are introduced to evaluate the MCDG system's performance compared to CDG systems. The unbiased realistic attitude of this research project toward the concept of multilateral closed loops helps to choose between CDG and MCDG systems for producing a particular amount of thermal power at a specific flow rate.

3. Based on extraction temperature and the ratio of generated thermal power to the equivalent total length, criteria are defined to optimize the operation/construction planning. The successful cases shall facilitate the design of future high-performance MCDG systems.

To achieve these objectives, the thermal transfer between different components of the system (i.e., circulating fluid, cement layer, casing, and formation) is accurately simulated. This advanced numerical modeling comprises of full coupling of mass, momentum, and energy equations, implementing equations of state (to account for variations of fluid density and viscosity as functions of pressure and temperature), modeling conductive heat transfer in a formation with the energy exchange inside the wellbores using an analytical radial heat exchange model, and superposing the lateral wellbores to decrease the computational cost.

2. System description

The extraction temperature of CDG is proportional to the heat output produced, but inversely proportional to the flow rate. Based on the previously conducted research by Esmaeilpour et al. [12], the highest possible amount of produced thermal power is smaller than ~2 MW$_t$, when operating with a CDG system possessing a total length of 12 km. Nevertheless, a larger heat exchange area can enhance the heat utilization capacity of the system and allows for operating with higher flow rates. Therefore, designing multilateral closed deep geothermal systems could be a suitable alternative to extending lateral heat exchange surfaces. In the following section, the structure of MCDG systems, introduced in this study, is elaborately explained.

2.1. General description of MCDG system

As shown in Fig. 1a, MCDG systems can possess several deep injection wellbores, which are joined through doglegs (a manifold) at a particular depth (Fig. 1a, point A). In a multilateral framework, it is important to maintain sufficient wellbore separation to prevent thermal interference between the different branches. Thermal interference can occur when the flow of working fluid from one branch of the system affects the temperature of the fluid in another branch, which can reduce the overall efficiency of the system. The optimum distance between these parallel wellbores is a function of time, thermo-physical properties, and temperature difference between wellbore and formation. The injected fluids through vertical wellbores are initially collected at these doglegs and then redistributed in horizontal wellbores. The total injected fluid is finally extracted through only one production wellbore. The uniform alteration of all the wellbores' diameters can change the heat exchange surface, cross-sectional area, fluid velocity, and convective heat transfer factor. However, it doesn't have a significant impact on the extraction temperature and generated thermal power [12]. So. It is reasonable to construct the system with small wellbore diameters ranging between 4″ and 12″ to decrease the relative drilling expenses. Nevertheless, operating with a smaller wellbore diameter increases the pressure loss due to friction. In order to avoid subsurface water contamination and preserve the system's integrity, the injection and production wellbores (i.e., vertical sections of the system) are equipped with several casings and cement layers. However, horizontal wellbores are sealed with some chemicals and directly exposed to hot formation [19]. Consequently, the circulating fluid experiences a greater pressure loss due to the larger friction factor of this section. However, this special design increases the leakage probability through the horizontal wellbores. Nevertheless, direct exposition to hot formation enhances the heat exchange rate dramatically as the thermal conductivity of the formation is much higher than that of cement. The conductive energy exchange between the circulating fluid and its surrounding area depends on the number of layers around the wellbore and their thermal conductivities. Embedding some cement layers with low thermal conductivity between the wellbore and its adjacent formation restricts thermal interaction severely. Therefore, removing casings and cement layers from the wellbore structure increases the overall thermal conductivity and heat absorption rate. As a result, this new devise of the system makes it feasible to capture a higher extraction temperature and improves thermal power generation. The circulating fluid exchanges energy with the wellbore completion system through convective heat transfer. This type of energy exchange depends on the fluid velocity. A higher fluid velocity increases the Reynolds and Nusselt numbers and considerably enhances the heat extraction rate.

2.2. Applied geological setting and geometrical configuration

In all the simulations of this study, the depth of the system is 4.1 km which includes the length of vertical wellbores and the depth of doglegs. The injection and production wellbores are located in two parallel
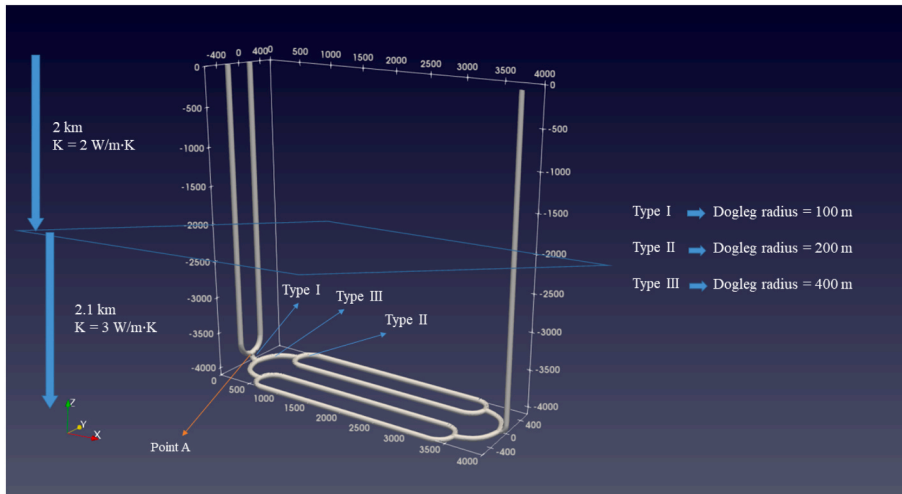
Fig. 1. Schematics illustrating a) depth of MCDG systems, length of horizontal section, doglegs and manifolds structure, and wellbores configuration b) casing program of a simple CDG system (b1 = 22″, c1 = 18 5/8″, b2 = 17″, c2 = 13 5/8″, b3 = 12 1/4″, c3 = 9 5/8″, b4 = 8 3/8″). b, c, Δz, and Δl stand for borehole diameter, casing inner diameter, depth of vertical wells, and total horizontal length, respectively. The horizontal section is directly exposed to hot formation. The same casing program is used for MCDG systems. The area highlighted by red color shows insulation.
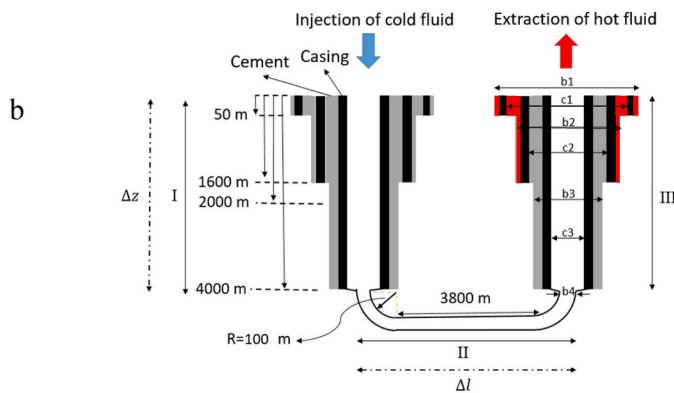
plates, which are 4 km away from each other (Fig. 1a). The MCDG system can possess 1, 2, 4, and 8 injection/horizontal wellbores that indicates the range of randomness for the number of wellbores in the stochastic analysis. This randomness is not attributed to the number of production wellbores as in all the simulations of this study only one production wellbore is included in the MCDG systems' structure. In order to preserve the 400 m distance between the parallel wellbores in both vertical and horizontal sections, they are connected to each other through some doglegs with radiuses of 100 m (type I), 200 m (type II), and 400 m (type III). This optimum distance (400 m) is calculated through analytical analysis [20] and some numerical simulations [5]. The casing program of vertical wellbores is addressed in Fig. 1b.

The thermal conductivities of casing, cement layer, and insulation material (urethane fiberglass) are 100 W m^{-1} K^{-1}, 0.7 W m^{-1} K^{-1}, and 0.021 Wm^{-1}K^{-1}, respectively [21]. The formation density is also supposed to be 2400 kg m^{-3}. The roughness of the inner casing in vertical wellbores is 10^{-4} m. However, due to the lack of casing in horizontal wellbores, the roughness of this section is assumed to be 2 × 10^{-4} m [22]. Two geological units with a depth of 2 km and 2.1 km comprise the formation that surrounded the system (Fig. 1a). The thermal conductivities of the upper and lower layers are 2 W m^{-1} K^{-1} and 3 W m^{-1} K^{-1}, respectively. The underground ambient temperature gradient is set to be 30 °C/km, and the surface temperature is 10 °C. Therefore, the undisturbed temperature in the deepest point of the system (4.1 km) is 133 °C (10 °C + 4.1 km × 30 °C/km = 133 °C).

3. Methodology

Accurate numerical modeling of MCDG systems should include a detailed description of energy exchange between wellbore and formation, heat transfer in formation, and transient processes in wellbores. Fluid flow inside the inner casing undergoes several coupled physical processes, such as pressure loss due to friction, kinetic energy alteration [23,24], temperature variation due to heat exchange with surrounding formation, velocity changes influencing pressure and temperature fields, and buoyancy effect because of variation of fluid density. In order to appropriately simulate these complex physical processes in a wellbore, a finite element code, called MOSKITO [11,25], is developed in the MOOSE (Multiphysics Object-Oriented Simulation Environment) Framework [26,27]. The capability and validity of this solver to model fluid flow and heat transfer in closed deep geothermal systems are assessed in another research project carried out by the authors of this study [12].

3.1. Governing equations

A non-isothermal transient flow in a pipe is governed by these equations [28]:

Continuity equation:

$$\frac{\partial}{\partial t}(\rho) = -\frac{\partial}{\partial z}(\rho v) + m \tag{1}$$

where ρ and v represent density and velocity of fluid, and m is the mass sink/source term in unit volume and unit time.

Momentum equation:

$$\frac{\partial P}{\partial z} = \rho g cos(\theta) \pm \frac{f \rho v^2}{2d} \pm \left(\frac{\partial}{\partial t}(\rho v) + \frac{\partial}{\partial z}(\rho v^2) \right) \tag{2}$$

where P, g, θ, f, and d refer to fluid pressure, gravitational acceleration, the inclination of the well, friction factor, and wellbore hydraulic

diameter, respectively. The sign of the right-hand side terms in the momentum equation depends on flow and gravity directions.

Energy equation:

$$\frac{\partial}{\partial t}\left[\rho\left(h - \frac{P}{\rho} + \frac{1}{2}v^2\right)\right] = -\frac{\partial}{\partial z}\left[\rho v\left(h + \frac{1}{2}v^2\right)\right] + \rho v g\cos(\theta) - \frac{q}{A} + Q \qquad (3)$$

where h, q and Q show the enthalpy, radial heat flow, and heat sink/source terms, respectively.

The main variables (i.e., flow rate, pressure, and enthalpy) are calculated by solving Eqs. (1)–(3). Some constitutive relationships/empirical equations, including viscosity, density, and the friction factor, are also required to solve these equations. The Vogel Equation [29] is used to calculate viscosity. Additionally, an empirical equation of state (EOS) [30] is implemented to compute the fluid density as a function of pressure, temperature, and salinity of the fluid (saline water).

Using a special radial heat exchange model makes it possible to simulate the heat exchange between the wellbore and its adjacent formation with a low computational cost. Based on this model, the radial heat flow can be calculated by:

$$q = 2\pi r_{to} U_{to}\left(T_f - T_{cf}\right) \qquad (4)$$

where r_{to}, U_{to}, T_f and T_{cf} indicate the outside radius of the inner tubing, the overall heat transfer coefficient, the fluid temperature, and the temperature at the cement/formation interface, respectively. For a detailed explanation, refer to Willhite [31].

3.2. Numerical modeling

Modeling several branches of MCDG systems can cause the simulation time to increase significantly. However, it should be taken into account that these lateral wellbores show a similar thermal/hydraulic behavior. Therefore, it is possible to simulate fluid flow and heat transfer for only one branch and assume the same pressure, temperature, and flow rate along other lateral wellbores. In order to apply this kind of superposition, a particular boundary condition is implemented, which receives the main variables at the end of the simulated branch in each time step and imposes the same pressure and temperature at the beginning of the subsequent section in the next time step. The boundary condition for the flow rate is also computed by the total volumetric flow rate divided by the number of branches.

The initial fluid temperature is set to be the same as the formation temperature, believing in an equilibrium thermal condition between residual fluid and its surrounding environment. The initial pressure condition is hydrostatic. Furthermore, Dirichlet boundary conditions with fixed values are imposed at the injection point for all variables. The injection temperature and pressure are 10 °C and 1 MPa, while the flow rate can take values between 5 and 50 l/s (i.e., range of flow rate randomness in the stochastic analysis), which will be mentioned for each simulation case.

A sensitivity analysis for three spatial discretizations ($\Delta x = 14$ m, $\Delta x = 11$ m, and $\Delta x = 7$ m) was conducted to confirm that the solution is mesh-independent. Evaluation of pressure and temperature fields over the length of the wellbores revealed the negligible impact of implemented mesh sizes on the results. The maximum variation of pressures and temperatures over their absolute values is less than 6×10^{-6} when changing the mesh size from 7 m to 14 m. Therefore the mesh size of 14 m was selected for the simulations to decrease the computational time. It is worth noting that increasing the mesh size to 25 m and 50 m leads to a greater relative variation in the main variables, up to 2×10^{-4} and 3×10^{-3}, respectively. The time steps gradually increase from 100 s to one month to provide a better convergence initially ($\Delta t = 100$ S) and subsequently decrease the simulation time ($\Delta t = 1$ month). The combination of superposition, reasonable time-stepping, and proper spatial discretization decreases the simulation time. Consequently, it takes less than 20 min to simulate 100 years of operation of an MCDG system using

a host PC with a 4-core CPU (Intel(R) Core(TM) 2 Quad) at 2.3 GHz.

4. Stochastic analysis of the MCDG system's long-term behavior

An accurate stochastic analysis of the system's long-term behavior supports the future design of high-performance MCDG systems and reduces the computational cost. Therefore, the main focus of this section is to find a meaningful correlation between long-term and short-term behaviours (values) of extraction temperature and generated thermal power as primary indicators of the system's performance. For this purpose, the behavior of 160 MCDG systems with 10 different flow rates (i. e., first arbitrary variable) and 16 various wellbore configurations (second arbitrary variable) is evaluated. As mentioned before, the flow rate randomness can range between 5 L/s and 50 L/s, while the number of vertical/horizontal wellbores can be 1, 2, 4, and 8.

Fig. 2 illustrates the extraction temperature and pressure in a simple CDG system with a depth of 4.1 km, horizontal length of 4 km, and flow rate of 5 L/s. Comparing Fig. 2a and b, it is evident that the overpressure ($\Delta P = P_{extraction} - P_{injection}$) tracks the trend of extraction temperature. In an isothermal condition, the extraction pressure is expected to be lower than the injection pressure due to friction loss. However, when fluid temperature is updated in non-isothermal simulations, a significant pressure increase occurs in the production wellbore. This is because the higher temperature of the working fluid in the production wellbore, along with the temperature-dependent density behavior, results in a lighter water column in the production side. This phenomenon, known as the thermosiphon effect, creates a pressure gradient between the vertical wellbores. The overpressure of approximately 2 MPa in Fig. 2b clearly indicates that the pressure rise caused by the density difference between the vertical wellbores is much greater than the pressure loss due to friction.

The operating flow rate can significantly influence the extraction temperature of closed-loop system. Fig. 3 shows the extraction temperature of a simple CDG system operating with a flow rate of 10 L/s. The immediate increase in extraction temperature was prompted by the displacement of residual hot fluid in wellbores. After this short period, the extraction temperature reduces due to the cooling down of the surrounded formation. For more information about the transient behavior of extraction temperature over time, refer to Esmaeilpour et al. [12].

Analogous to Fig. 3, the transient behavior of extraction temperature for 160 MCDG systems with various flow rates and wellbore configurations is analyzed. Fig. 4 shows the extraction temperatures after 1 year, 30 years, and 100 years. This figure consists of two main sections. Each section contains a parabola fitting of 160 points representing the extraction temperatures of simulated cases. The right curve exhibits the temperature of the produced fluid after 30 years of operation as a function of the extraction temperature at the end of the first year of the operation. The left curve shows the extraction temperatures after 30 years and 100 years. For example, the extraction temperatures of a simple case with a flow rate of 10 L/s (Fig. 3) are marked with arrows in Fig. 4 to explain how to use/read the figure. Points 1, 2, and 3 in Fig. 4 correspond to the extraction temperatures in Fig. 3 for the mentioned operation year (1, 30 and 100) as a temporal instance. Similarly, the extraction temperatures of other MCDG systems are included in this figure. Since the left and right sections share one of their axes (i.e., the axis which indicates the extraction temperature after 30 years), it is also possible to read the temperature of produced fluid after one century of operation based on the extraction temperature after the first year and vice versa.

In contrast to the nonlinear change of T_{30} as a function of T_1 (Fig. 4, right side), the relationship between T_{30} and T_{100} (Fig. 4, left side) is almost linear. These correlations between extraction temperatures over different periods are in good agreement with the observed trend of extraction temperature in other studies. Esmaeilpour et al. [12] showed that the extraction temperature of CDG systems experiences a huge
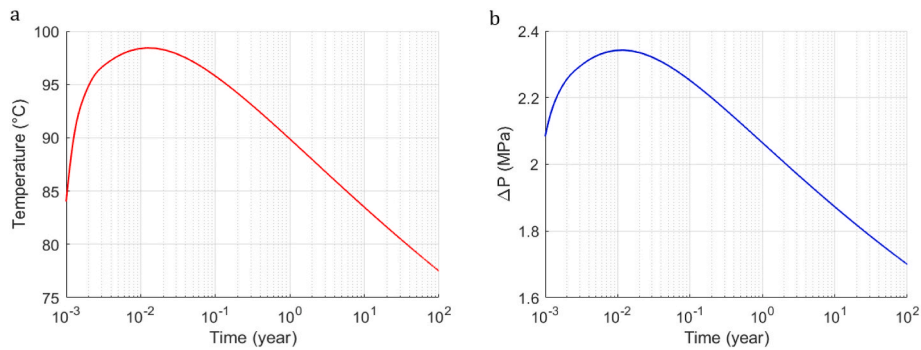
Fig. 2. The transient behavior of a) extraction temperature b) extraction pressure, for a simple CDG system with a depth of 4.1 km, horizontal length of 4 km, and flow rate of 5 L/s. ΔP is defined by ($\Delta P = P_{extraction} - P_{injection}$).
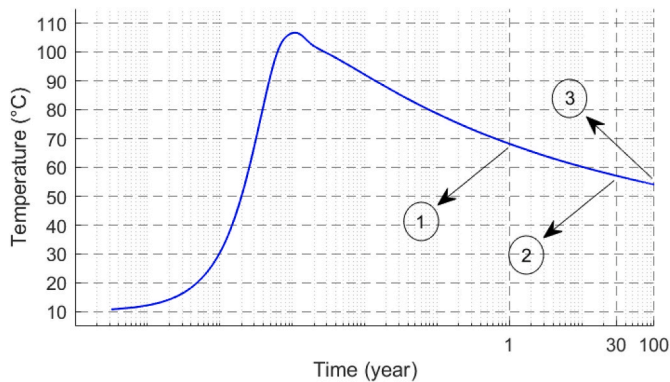

Fig. 3. Behavior of extraction temperature over time while operating with a simple CDG system. The flow rate is 10 L/s and other initial/boundary conditions and casing program are mentioned in sections 2 and 3. Points 1, 2, and 3 correspond to extraction temperatures after 1, 30, and 100 years, respectively.
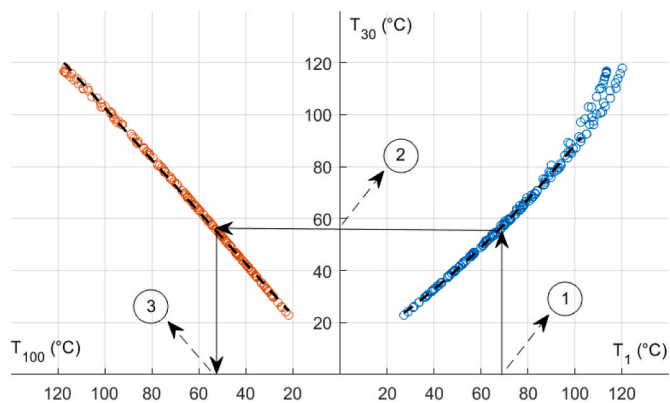

Fig. 4. Correlations between extraction temperatures of MCDG systems after 1 year, 30 years, and 100 years of operation.

nonlinear temperature change initially, and then it undergoes a small (linear) variation over time. The provided example in Fig. 3 also shows the same behavior that the extraction temperature decreases 11 °C in the period of 1–30 years, while its reduction is less than 3 °C in the period of 30–100 years. Moreover, the maximum observed reduction of extraction temperature in 30–100 years is approximately 4 °C, which shows the longevity of MCDG systems. This remarkable longevity is also represented by the inclination angle of T_{100} over T_{30} (45°), implying that the extraction temperature after 100 years is almost equal its value after 30 years of operation.

It is also worth mentioning that there is no clear relation between the

extraction temperatures when T_1 is higher than 105 °C. Operating with low flow rates leads to the temperature increment of the working fluid entering the production wellbore. This hot fluid experiences a considerable temperature drop in the production wellbore. Nevertheless, as reported by Esmaeilpour et al. [12], heating the area around the production wellbore prevents the temperature drop along this wellbore and results in extraction temperature enhancement over time. This strange behavior of extraction temperature causes deviation from the parabola fitting.

In Fig. 5, the energy density (i.e., extracted energy per liter of circulating fluid) over the project lifetime of one hundred years is plotted versus the extraction temperature after the first year. Using the energy density for the calculation of total generated thermal power (power (MW$_t$) = energy density (MJ/L) × flow rate (L/s)) should be treated with care. As shown in Fig. 5, only low flow rates can result in high extraction temperature after the first year (T_1). However, small extraction temperatures can be outcomes of either low or high flow rates. Therefore, the provided colormap shows the maximum allowed flow rate for the calculation of thermal power. The provided example in Fig. 5 shows the calculation procedure clearly. When the extraction temperature after the first year (T_1) is 84 °C, the energy density is 0.26 MJ/L. Calculation of average generated thermal power requires reading the flow rate from the colormap. For the energy density of 0.26 MJ/L, the flow rate is 40 L/s, leading to the total thermal power production of 10.4 MW$_t$ (0.26 MJ/L × 40 L).
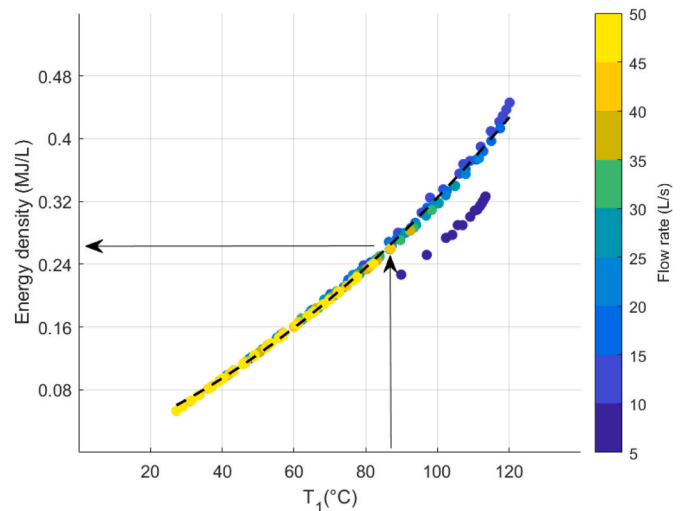

Fig. 5. Correlations between extraction temperatures of MCDG systems after 1 year and extracted energy per liter of working fluid over 100 years of operation. The provided colormap shows the maximum allowed flow rate for the calculation of thermal power.

In conclusion, the achieved relation between short-term and long-term values of extraction temperature is independent of flow rate and the number of wellbores. It shows the possibility of utilizing these correlations to anticipate the performance of other MCDG systems with various flow rates and wellbore configurations. It should be noted that the depth of the system, length of horizontal wellbore, number of casing/cement layers around wellbores, thermo-physical properties of geological layers, and subsurface temperature gradient can influence the short-term behavior of the system. Nevertheless, the long-term behavior of the system will be again a specific function of its short-term performance. For example, the temperature of extracted fluid after 100 years of operation can still be anticipated as a linear function (different slope) of the extraction temperature after 30 years. The spacing of the lateral wellbores could affect this correlation. If the well spacing is reduced below 400 m (i.e., the distance that ensures no thermal interference), it will inevitably lead to a different correlation. This is because reducing the spacing further will lower production temperatures in long-term behavior. In this study, a well spacing of 400 m is used to ensure no thermal interaction between parallel wellbores and maximize energy absorption from the reservoir.

5. Results

5.1. General behavior of MCDG systems

Based on the previous investigations conducted by Esmaeilpour et al. [12], operating with high flow rates reduces the extraction temperature of CDG systems and violates their longevity. On the other hand, the low range of operating flow rates limits the system's power production as the maximum generated thermal power of the designed CDG system was approximately 2 MW$_t$. Therefore, the primary purpose of this section is to evaluate the impact of multiple wellbores on the thermal power generation, heat absorption rate and, extraction temperature.

Analogous to section 4, 160 different MCDG systems are designed to perform stochastic analysis with regard to flow rate and system configuration. Their geometrical configuration, parameters and BCs/ICs are addressed in sections 2 and 3, respectively. In order to have a meaningful comparison of different cases, an index called *specific power* (W/m) is defined as the ratio of the generated thermal power to the equivalent total length of the system:

$$specific\ power = \frac{generated\ power}{equivalent\ total\ length} \quad (5)$$

where the equivalent total length is a simplified/normalized indicator of drilling expenses, defined by this equation:

$$Equivalent\ total\ length = total\ length\ of\ vertical\ wellbores + 2$$
$$\times total\ length\ of\ horizontal\ wellbores \quad (6)$$

It is assumed that the horizontal wellbore's drilling cost is two times that of a vertical wellbore. However, this weighting coefficient can be changed considering the length of the wellbores, their diameters, geological condition, casing program, drilling technology, and other complicated parameters. The calculated specific power of a simple CDG system operating with a flow rate of 5 L/s is 70.81 W/m [12]. Accordingly, the specific power >70.81 W/m is an indicator of a more productive system compared to the CDG system resulted in shortening the relative payback period. Therefore, it is technically reasonable to operate with MCDG systems possessing a specific power of >70.81 W/m. However, this criterion should not be considered a sharp indicator for project decision making.

Fig. 6 exhibits the impact of flow rate on the average values of extraction temperature, generated thermal power, and specific power over 100 years of operation. As mentioned before, 16 various configurations are modeled for each flow rate. Therefore, the boxplots show the impact of multiple wellbores at a specific flow rate. The increment of the
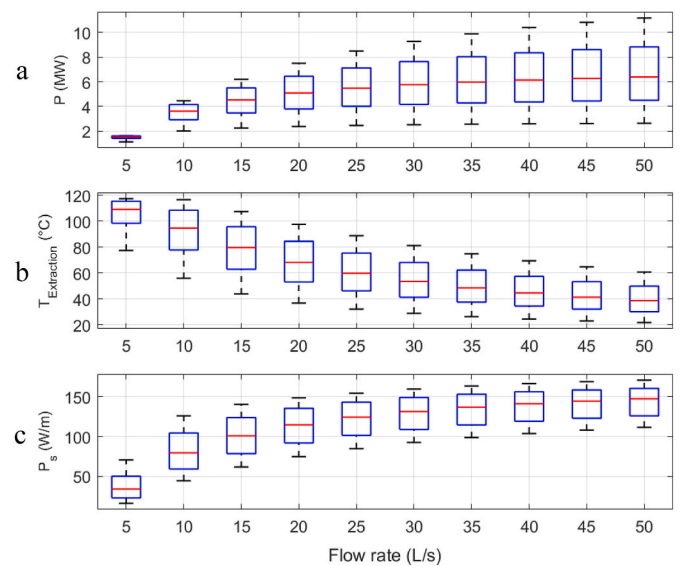

Fig. 6. Ranges of generated thermal power (P), average extraction temperature over 100 years of operation ($T_{Extraction}$), and specific power (P_S) for each flow rate. The boxplots show the impact of wellbore configurations at each flowrate.

flow rate enhances the thermal power generation and the specific power. Although the extraction temperature and the generated thermal power are very sensitive to low flow rates, their sensitivity to high flow rates is negligible (Fig. 6a). As an example, median, lower/upper quartiles and whiskers of generated thermal powers at the flow rate of 45 L/s are almost the same as those of 50 L/s. It indicates that for the simulated set of system configurations, the decline of extraction temperature compensates for the increment of operating flow rate, leading to a small variation in the generated thermal power spectrum. Consequently, exceeding a critical value of flow rate reduces the extraction temperature and doesn't change the generated thermal power significantly compared to its variation at lower flow rates. However, it should be high enough to exploit the maximum potential of the system. It is also shown that the increase in flow rate is associated with higher uncertainty in the determination of power production (Fig. 6a). For instance, adding extra wellbores increases the generated thermal power of the system from 3.5 MW$_t$ to 10 MW$_t$, when the flow rate is 35 L/s. Although operating with multilateral systems can scale up the thermal power production at high flow rates, the increase in the number of wellbores seems to be unreasonable when operating with low flow rates since the generated thermal power doesn't increase significantly (Fig. 6a, flow rate = 5 L/s). Finally, increasing the flow rate reduces the extraction temperature significantly (Fig. 6b). Consequently, the reduction of extraction temperature and low sensitivity of generated thermal power to high flow rates are the main barriers to the increase of flow rate.

Fig. 7 shows the impact of system configuration on the extraction temperature, generated thermal power, and specific power of various MCDG systems consisting of 10 flow rates ranging between 5 L/s and 50 L/s. Therefore, the boxplots show the impact of flow rates for each system configuration. The first and second indices of each configuration show the number of injection and horizontal wellbores, respectively (e. g. the configuration of 2:4 means 2 injection and 4 horizontal wellbores).

As shown in Fig. 7, adding extra horizontal wellbores is more impactful than including additional injection wellbores to enhance power production and extraction temperature. Indeed, the working fluid is directly exposed to the hottest formation in the horizontal wellbore. Hence, this part of the system is very important for heat absorption. This finding is also testified by Esmaeilpour et al. [12], that the magnitude and behavior of net generated thermal power is like the power production in the horizontal wellbore of CDG systems. Nevertheless, the
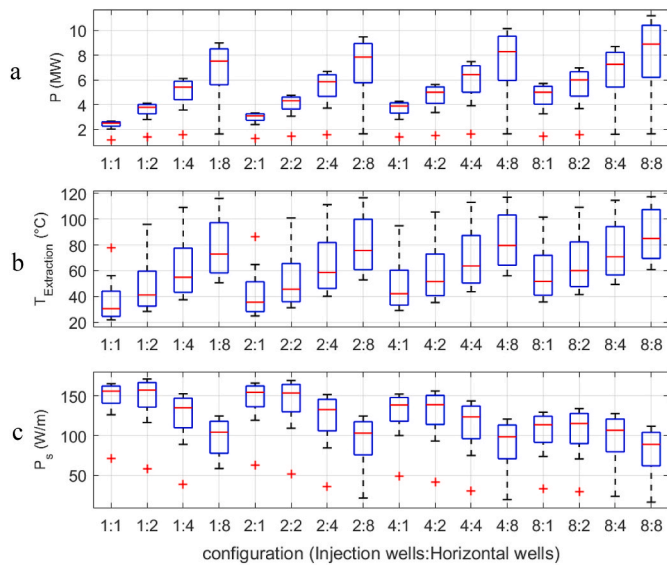
Fig. 7. Ranges of generated thermal power (P), average extraction temperature over 100 years of operation ($T_{Extraction}$), and specific power (P_S) for wellbore configuration. The domain of boxplots shows the impact of flow rate on outputs. The first and second indexes of each configuration show the number of injection and horizontal wellbores, respectively.

high relative drilling cost is a primary obstacle to increasing the number of horizontal wellbores since it increases the equivalent total length of the system and subsequently reduces the specific power. Therefore, the increment of produced thermal power and the excess drilling expenses are the primary criteria that should be considered when adding a new horizontal wellbore to an MCDG system.

5.2. Suggestion of appropriate operation plans

Utilizing MCDG systems doesn't guarantee a better performance compared to CDG systems as demonstrated in section 5.1. Finding a high-performance MCDG system is a key issue for a successful project. Therefore, this section is dedicated to filtering out inappropriate cases (from our 160 models) which are not aligned with sustainable and profitable geothermal production. Furthermore, the important outcome will be the identifying of specific shared features in all filtered cases to make the study transferable.

Fig. 8 illustrates the total generated thermal power, average extraction temperature over 100 years of operation, and the specific power of each simulated case. Increasing the number of wellbores and the reduction of the total flow rate result in a higher extraction temperature (the top left quarter in Fig. 8.). However, both factors typically lead to a lower specific power due to either decreasing the generated thermal power or increasing the equivalent total length of a system. As a result, the studied MCDG systems are not capable of producing electric power cost-effectively (it is worth mentioning that a deeper system or longer horizontal section may make electric power generation feasible but it is out of the scope of the current study). Nonetheless, they are potentially reliable for district heating purposes. On the other hand, operating with a higher flow rate increases the generated thermal power and enhances the specific power, but it reduces the extraction temperature (the bottom right quarter in Fig. 8.). To conclude, it is crucial to set criteria, in which high specific power and extraction temperatures coincide, to choose proper operation/construction plans. In this study, the cases with the extraction temperature >60 °C (the min temperature suitable for district heating) and the specific power >70.81 W/m (the specific power of the CDG system introduced earlier) are assumed to be convenient for operation and named successful cases. Remarkably, the majority of the selected cases (the grey rectangle in Fig. 8.) also have
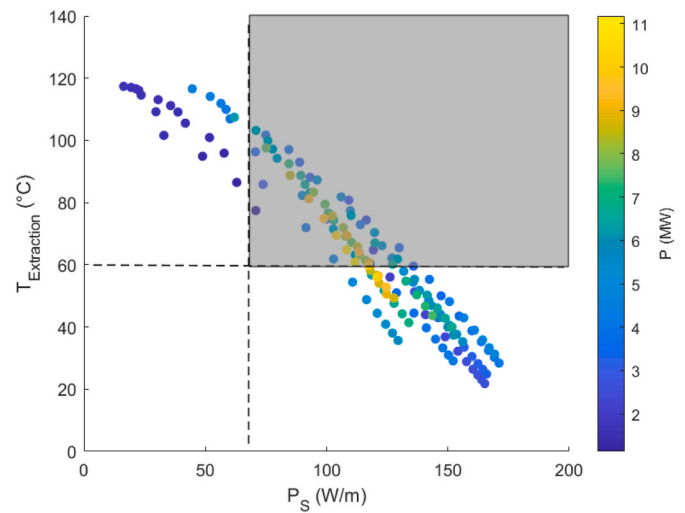

Fig. 8. Average values of extraction temperature over 100 years of operation ($T_{Extraction}$), specific power (P_S), and total generated power (P) of each case. The plotted lines show the filtering criteria (average extraction temperature >60 °C and specific power >70.81 W/m). The points located in the grey region are successful cases.

higher generated thermal power than the disregarded cases. The MCDG systems with an extraction temperature range of 60 °C–100 °C (successful cases) are well-suited for use in district heating and local heating applications to provide warmth to buildings. The main difference between these two applications is in the scale of the system and how heat is distributed. Geothermal district heating is a large-scale system that distributes heat to entire neighborhoods or cities through a network of pipes that carry hot water or steam, while local heating is a smaller-scale system that provides heat to individual buildings or homes using boilers or heat pumps. The typical temperature range of geothermal fluids used for district heating is between 70 and 120 °C [32]. The flow rate for district heating systems can vary widely depending on the size of the system and the demand for heat. According to a report by the international energy agency [33], the flow rate for district heating networks in Europe ranges from less than 1 L/s for small networks to more than 50 L/s for large networks. In contrast, the typical temperature range for local heating systems depends on the type of heating equipment used. According to the U.S. department of energy [34], the temperature range for hot water boilers is typically 40–80 °C. The local heating network in Riehen (a municipality in the canton of Basel-Stadt in Switzerland) is a good example of local heating where geofluid with a temperature of 66 °C is heated with the help of a heat pump to provide hot fluid with a temperature of 80–90 °C to dwellings at a flow rate of 25 L/s [35]. The extraction temperature and flow rate of successful MCDG systems clearly demonstrate their capability to be used for both district heating and local heating applications.

Fig. 9 exhibits the total flow rates and wellbore configurations of successful cases highlighted in Fig. 8. Clearly, the points are clustered with a specific repeated pattern and oriented toward the right side (of the pattern), where the MCDG system possesses more lateral wellbores. It indicates that by increasing the number of wellbores, it is more likely to have a successful case (this assessment doesn't include drilling difficulties). What are the common features of these repeated patterns? Finding these features in successful cases supports a better design of high-performance MCDG systems in the future. Therefore, it is tried to find a meaningful correlation between local parameters (flow rates per injection/horizontal wellbores) and global parameters (i.e. specific power, average extraction temperature, and total flow rate of successful cases).

Fig. 9 plots flow rates per injector and lateral for successful cases, and global parameters are shown in each subfigure. Flow rates per injector
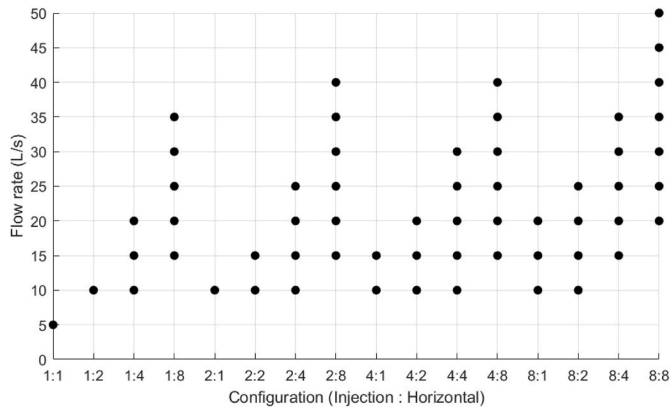
Fig. 9. Flow rates and corresponding configurations of successful cases. The first and second indexes of each configuration show the number of injection and horizontal wellbores, respectively.

and lateral are calculated by dividing the total operating flow rate by the number of injection and horizontal wellbores, respectively. The main outcome is that the plotted data has an upper limit (asymptote) which is governed by:

$$flow\,rate\,per\,lateral < \frac{1}{a \times (flow\,rate\,per\,injector)^2 + b \times (flow\,rate\,per\,injector) + c}$$

(7)

where a, b, and c are −3.16e-4, 1.69e-2 and -3.85e-3, respectively. These factors are specific to this study, and they vary in different geometrical/ geological conditions.

The extraction temperature is decreasing along the arrows shown in Fig. 10a and b while the specific power is increasing. All plotted points under the curve have an extraction temperature of higher than 60 °C, demonstrating that the extraction temperature is the main factor forming Eq. (7). Additionally, it is found that high total flow rates are achievable when the flow rate per injector is approximately the same as the flow rate per lateral (Fig. 10c). Simultaneous low flow rates per injector and lateral can guarantee a high extraction temperature. However, the points with low flow rates per lateral possess higher extraction temperatures compared to the points with low flow rates per injector. Therefore, horizontal wellbores are preferable to vertical wellbores in terms of extraction temperature enhancement due to the direct exposition of working fluid to hotter formation in the horizontal section. Consequently, to maximize the extraction temperature, the number of horizontal wellbores should be certainly higher than the number of injection wellbores. However, a high extraction temperature cannot guarantee considerable thermal power production. Moreover, the increase in the total flow rate necessitates operating with MCDG systems in which the number of injection wellbores is roughly equal to the number of horizontal wellbores. Hence, contrary to conventional belief, it is not a good idea to construct an MCDG system with only one injection wellbore and many horizontal wellbores. Nonetheless, the number of horizontal wellbores should be higher than the number of injection wellbores.

Fig. 11 shows the success rate calculated by dividing the number of successful cases by the total number of simulated cases for each flow rate (i.e., 16 configurations). The highest success rate occurs when the flow rate ranges between 10 L/s and 25 L/s. For instance, the success rate is 75% when the flow rate is 15 L/s. Small generated thermal power and low extraction temperature make it risky to operate with low and high flow rates in MCDG systems, respectively.

6. Conclusion

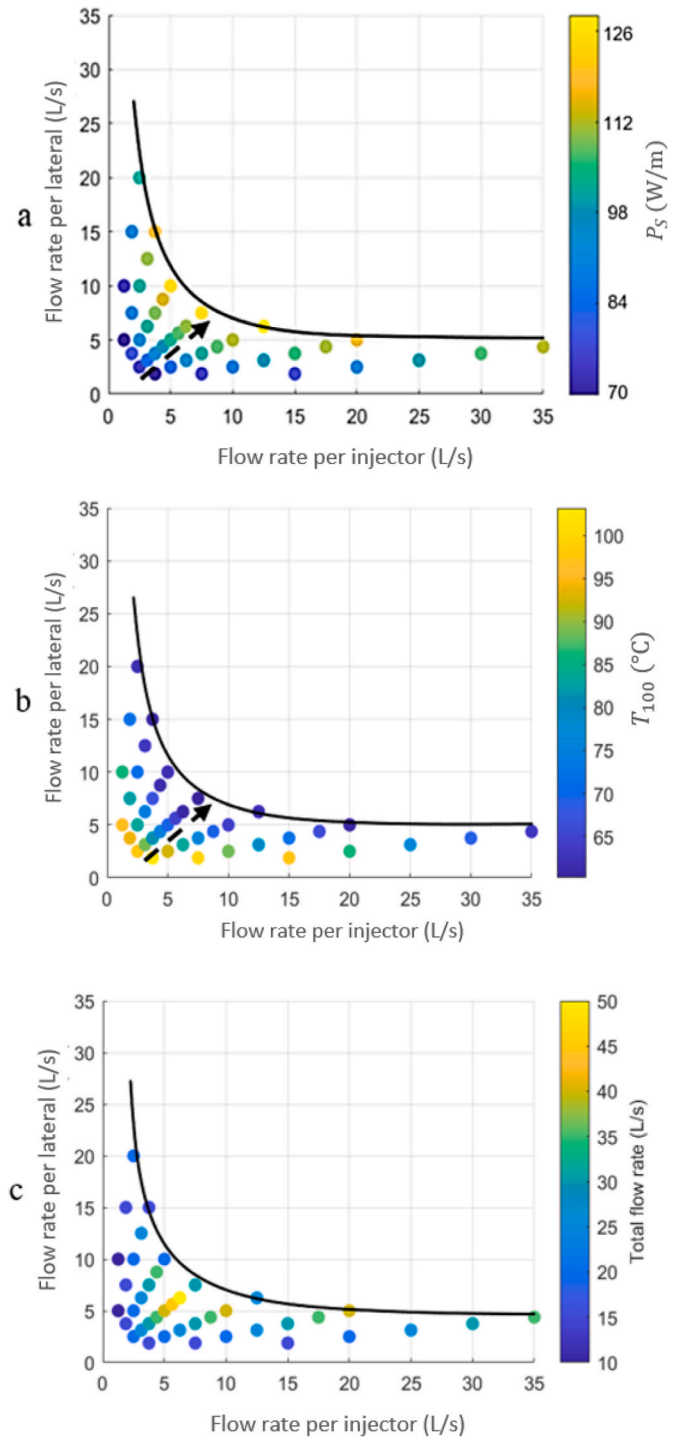Designing high-performance MCDG systems makes it feasible to

Fig. 10. Correlation between flow rates per lateral/injector and a) specific power b) average extraction temperature over 100 years of operation c) total flow rate (L/s).

obtain baseload power in an environmentally friendly manner without causing seismic events and contaminating subsurface water. Therefore, the main purposes of this study were to analyze the heat extraction capability of MCDG systems, enhance their performance, and increase their contribution to green energy generation. To achieve these targets, several multilateral systems with various operational parameters and configurations are proposed. In the first step, the system's long-term performance is described as a function of its short-term behavior through stochastic analysis. This way, the short-term outputs (i.e.,
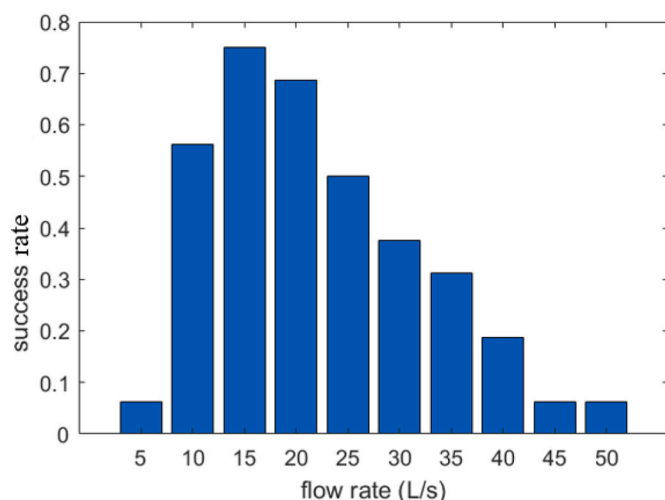
Fig. 11. Success rate of designed MCDG systems for each flow rate (*success rate = number of sucessful cases at each flow rate*/16).

extraction temperature and generated thermal power) and appropriate operational/configurational parameters can be back-calculated out of the desired long-term performance. Then, the impact of flow rate and wellbore configuration on the system's behavior is assessed. Defining a specific power allows comparing the performance of individual MCDG systems. The ratio of generated thermal power to the equivalent total length of the system is of key importance for economic analyses. It is concluded that the performance of MCDG systems is not always better than simple CDG systems. Subsequently, some criteria are set to select the best operation/configuration plans. Finally, the common features of successful cases are characterized, which gives insight into designing high-performance MCDG systems.

The key findings of this study are listed below.

1. It is found that the long-term extraction temperature and generated thermal power of MCDG systems can be predicted as functions of their short-term extraction temperature through stochastic analysis. Interestingly, these correlations are independent of the number of wellbores and flow rate.
2. Operating with MCDG systems doesn't always result in better performance than CDG systems. It is also demonstrated that adding horizontal wellbores is more beneficial than including extra injection wellbores in terms of power production.
3. The findings of this study revealed that regardless of technical drilling difficulties, increasing the number of lateral wellbores enhances the heat absorption per meter of the system and the success rate.
4. The cases with appropriate extraction temperate and high ratio of generated thermal power to the equivalent total length can be characterized by a specific relation between flow rates per injection and horizontal wellbores.
5. In contrast to conventional belief, it is not reasonable to operate with only one injection wellbore and many horizontal wellbores since the highest total flow rate is achievable when the flow rate per injector approaches the flow rate per lateral.

The quantitative results of the present work provide a realistic overview of the heat extraction potential of MCDG systems. Nevertheless, the drilling expense is another essential factor that should be taken into account when selecting the best system design. In this study, a specific criterion is defined to give a rough estimation of the ratio of thermal power to relative drilling costs. However, future research should focus more on various drilling technologies and associated costs/ risks to improve the defined criterion and provide a comprehensive economic analysis. It is also worth mentioning that the structure of

doglegs and manifolds may be more complicated in real MCDG systems. This complexity cannot considerably change the energy absorption of the system as the length of the doglegs is small compared to the total length of the system. Nonetheless, dogleg design is an important topic for future studies concerning the drilling of MCDG systems.

CRediT authorship contribution statement

Morteza Esmaeilpour: Investigation, Methodology, Validation, Writing – original draft, Visualization. **Maziar Gholami Korzani:** Methodology, Writing – review & editing, Supervision. **Thomas Kohl:** Writing – review & editing, Supervision, Project administration.

Declaration of competing interest

The authors declare that they have no known competing financial interests or personal relationships that could have appeared to influence the work reported in this paper.

References

[1] J. Formhals, F. Feike, H. Hemmatabady, et al., Strategies for a transition towards a solar district heating grid with integrated seasonal geothermal energy storage, Energy 228 (2021), 120662.
[2] Y. Chen, J. Wang, P.D. Lund, Sustainability evaluation and sensitivity analysis of district heating systems coupled to geothermal and solar resources, Energy Convers. Manag. 220 (2020), 113084.
[3] X. Zhang, Numerical study of geothermal district heating from a ground heat exchanger coupled with a heat pump system, Appl. Therm. Eng. 185 (2021), 116335.
[4] C. Clauser, M. Ewert, The renewables cost challenge: levelized cost of geothermal electric energy compared to other sources of primary energy – review and case study, Renew. Sustain. Energy Rev. 82 (2018) 3683–3693.
[5] K. Stricker, J.C. Grimmer, R. Egert, et al., The potential of depleted oil reservoirs for high-temperature storage systems, Energies 13 (24) (2020) 6510.
[6] M. Gholami Korzani, S. Held, T. Kohl, Numerical based filtering concept for feasibility evaluation and reservoir performance enhancement of hydrothermal doublet systems, J. Petrol. Sci. Eng. 190 (2020), 106803.
[7] R. Egert, M.G. Korzani, S. Held, et al., Implications on large-scale flow of the fractured EGS reservoir Soultz inferred from hydraulic data and tracer experiments, Geothermics 84 (2020), 101749.
[8] E. Gaucher, M. Schoenball, O. Heidbach, et al., Induced seismicity in geothermal reservoirs: a review of forecasting approaches, Renew. Sustain. Energy Rev. 52 (2015) 1473–1490.
[9] A. Dhar, M.A. Naeth, P.D. Jennings, et al., Geothermal energy resources: potential environmental impact and land reclamation, Environ. Rev. 28 (4) (2020) 415–427.
[10] T.D. Rathnaweera, W. Wu, Y. Ji, et al., Understanding injection-induced seismicity in enhanced geothermal systems: from the coupled thermo-hydro-mechanical-chemical process to anthropogenic earthquake prediction, Earth Sci. Rev. 205 (2020), 103182.
[11] M. Esmaeilpour, M. Gholami Korzani, T. Kohl, Performance Analyses of Deep Closed-Loop U-Shaped Heat Exchanger System with a Long Horizontal Extension: 46th Workshop on Geothermal Reservoir Engineering, Stanford University, Stanford, California, 2021.
[12] M. Esmaeilpour, M. Gholami Korzani, T. Kohl, Impact of thermosiphoning on long-term behavior of closed-loop deep geothermal systems for sustainable energy exploitation, Renew. Energy 194 (2022) 1247–1260.
[13] X. Gao, Y. Zhang, Y. Huang, et al., Study on heat extraction considering the number and orientation of multilateral wells in a complex fractured geothermal reservoir, Renew. Energy 177 (2021) 833–852.
[14] Y. Shi, X. Song, G. Wang, et al., Study on wellbore fluid flow and heat transfer of a multilateral-well CO2 enhanced geothermal system, Appl. Energy 249 (2019) 14–27.
[15] G. Song, X. Song, G. Li, et al., An integrated multi-objective optimization method to improve the performance of multilateral-well geothermal system, Renew. Energy 172 (2021) 1233–1249.
[16] X. Song, Y. Shi, G. Li, et al., Numerical simulation of heat extraction performance in enhanced geothermal system with multilateral wells, Appl. Energy 218 (2018) 325–337.
[17] G. Wang, X. Song, Y. Shi, et al., Comparison of production characteristics of various coaxial closed-loop geothermal systems, Energy Convers. Manag. 225 (2020), 113437.

[18] G. Wang, X. Song, Y. Shi, et al., Heat extraction analysis of a novel multilateral-well coaxial closed-loop geothermal system, Renew. Energy 163 (2021) 974–986.

[19] Eavor, The First Truly Scalable Form Of Clean Baseload Power 10/4 (2021). https://www.eavor.com/.

[20] H.J. Ramey, Wellbore heat transmission, J. Petrol. Technol. 14 (1962) 427–435, 04.

[21] H. Tang, B. Xu, A.R. Hasan, et al., Modeling wellbore heat exchangers: fully numerical to fully analytical solutions, Renew. Energy 133 (2019) 1124–1135.

[22] I.E. Idelchik, Handbook of Hydraulic Resistance, 1996. New York.

[23] M. Esmaeilpour, M. Gholami Korzani, Enhancement of immiscible two-phase displacement flow by introducing nanoparticles and employing electro- and magneto-hydrodynamics, J. Petrol. Sci. Eng. 196 (2021), 108044.

[24] M. Esmaeilpour, M. Gholami Korzani, Analyzing impacts of interfacial instabilities on the sweeping power of Newtonian fluids to immiscibly displace power-law materials, Processes 9 (5) (2021) 742.

[25] M. Gholami Korzani, F. Nitschke, S. Held, et al., The development of a fully coupled wellbore-reservoir simulator for geothermal application, Trans. Geoth. Resour. Counc. 43 (2019) 927–936.

[26] D. Gaston, C. Newman, G. Hansen, et al., MOOSE: a parallel computational framework for coupled systems of nonlinear equations, Nucl. Eng. Des. 239 (10) (2009) 1768–1778.

[27] C.J. Permann, D.R. Gaston, D. Andrs, et al., MOOSE: enabling massively parallel multiphysics simulation, Software 11 (10) (2020), 100430.

[28] S. Livescu, L.J. Durlofsky, K. Aziz, et al., A fully-coupled thermal multiphase wellbore flow model for use in reservoir simulation, J. Petrol. Sci. Eng. 71 (3–4) (2010) 138–146.

[29] M.J. Assael, S.A. Monogenidou, M.L. Huber, et al., New international formulation for the viscosity of heavy water, J. Phys. Chem. Ref. Data 50 (3) (2021), 33102.

[30] S. Phillips, A. Igbene, j. Fair, et al., A Technical Databook for Geothermal Energy Utilization, Lawrence Berkeley National Laboratory, 1981.

[31] G.P. Willhite, Over-all heat transfer coefficients in steam and hot water injection wells, J. Petrol. Technol. 19 (1967) 607–615, 05.

[32] A.R. Mazhar, S. Liu, A. Shukla, A state of art review on the district heating systems, Renew. Sustain. Energy Rev. 96 (2018) 420–439.

[33] IEA, International Energy Agency, IEA (2023). https://www.iea.org/.

[34] DOE, "U.S, department of energy, https://www.energy.gov/.

[35] Schädle Karl-Heinz, Fernwärme und Geothermie Praxisbeispiel Riehen, 2015.